TECH. NOTE
R.P.D.51

TECH. NOTE
R.P.D.51

UNCLASSIFIED

~~SECRET~~

ROYAL AIRCRAFT ESTABLISHMENT

FARNBOROUGH, HANTS

TECHNICAL NOTE No: R.P.D.51

INVESTIGATION OF
ROUGH RUNNING OF A ROCKET BURNER
AND OBSERVATIONS ON
"SHORT TUBE" INJECTION ORIFICES

by

R.P.HAGERTY, Ph.D. and F.C.JESSEN,

ROCKET PROPULSION DEPARTMENT, WESTCOTT

EXCLUDED FROM AUTOMATIC REGRADING;
DOD DIR 5200.10 DOES NOT APPLY

Reviewed 19 67 PICATINNY ARSENAL
Retain Present Classification
Downgrade to
Destroy INVENTORY 1972

11. THIS INFORMATION IS DISCLOSED FOR OFFICIAL USE BY THE RECIPIENT GOVERNMENT. DISCLOSURE TO ANY OTHER GOVERNMENT OR RELEASE TO THE PRESS OR IN ANY OTHER WAY WOULD BE A BREACH OF THIS CONDITION.

2. THE INFORMATION SHOULD BE SAFEGUARDED UNDER RULES DESIGNED TO GIVE THE SAME STANDARD OF SECURITY AS THAT MAINTAINED BY HIS MAJESTY'S GOVERNMENT IN THE UNITED KINGDOM.

3. THE INFORMATION CONTAINED IN THIS REPORT SHOULD NOT BE CIRCULATED OUTSIDE GOVERNMENT DEPARTMENTS WITHOUT THE PRIOR PERMISSION OF THE MINISTRY OF SUPPLY.

MINISTRY OF SUPPLY

THIS DOCUMENT IS THE PROPERTY OF H.M. GOVERNMENT AND ATTENTION IS CALLED TO THE PENALTIES ATTACHING TO ANY INFRINGEMENT OF THE OFFICIAL SECRETS ACT, 1911-1939.

It is intended for the use of the recipient only, and for communication to such officers under him as may require to be acquainted with its contents in the course of their duties. The officers exercising this power of communication are responsible that such information is imparted with due caution and reserve. Any person other than the authorised holder, upon obtaining possession of this document, by finding or otherwise, should forward it, together with his name and address, in a closed envelope to:-

THE SECRETARY, MINISTRY OF SUPPLY. MILLBANK, LONDON, S.W.1.

Letter postage need not be prepaid, other postage will be refunded. All persons are hereby warned that the unauthorised retention or destruction of this document is an offence against the Official Secrets Act

REVIEW ON June 81

21060-57-001
~~6642038S8~~

~~SECRET~~ Best Available Copy
UNCLASSIFIED

52AA-4336

U.D.C. No. 621.455.013.4

10 Technical Note No. R.P.D.51

6 June, 1951

2 ROYAL AIRCRAFT ESTABLISHMENT, FARNBOROUGH

4 Investigation of Rough Running of a Rocket Burner and Observations on "Short Tube" Injection Orifices

by

R.P. Hagerty, Ph.D.
F.C. Jessen

Rocket Propulsion Department, Westcott

SUMMARY

The elbow approach to the inner circle of nitric acid orifices in an impinging jet type nitric acid - kerosene burner was thought to be responsible for the poor spray characteristics and consequent rough combustion. Water flow tests with a test piece shewed that the actual cause lay in the inclination of the entry face of each individual orifice to the axis of the orifice This caused dispersion and deflection of the issuing jets and impingement was impaired.

Further tests spotlighted the importance of the contour of the entry to the "short tube" type of orifice - this should be radiused for best results. In addition, the approach to the entry should be as direct as possible. The existence of a discontinuity in the curve of discharge coefficient against injection pressure was observed for all forms of entry contour other than fully radiused. A method of calculating the transition pressure for any liquid injected through an orifice of any diameter is suggested.

---

1. Nitric acid
2 Kerosene
3. Injectors

I Hagerty, R.P.

LIST OF CONTENTS

LIST OF APPENDICES

LIST OF ILLUSTRATIONS

LIST OF ILLUSTRATIONS (Contd.)

1 Introduction

During water flow testing of two rocket motor burners of the two to one impinging jet type of generally similar design, a marked difference was noticed in the spray patterns. The jets from the orifices in burner NA7, Fig.1a, were clean and impinged accurately, producing a well atomized and uniformly distributed spray. With burner NA12, Fig.1b, the jets from the inner circle of orifices were disperse, impingement was impaired, and the resultant spray was indifferently atomized and unevenly distributed. In firings with nitric acid and kerosene as propellants, burner NA7 gave smooth ignition and combustion with the flame front stable at a short distance from the face of the burner, whereas with burner NA12 the reverse was the case, ignition and combustion being noticeably rough.

Inspection of the orifices in burner NA12 for drilling defects, for example burrs on entry or exit edges, revealed no reason for the poor injection characteristics. Comparison of the designs shewed that the only difference of significance lay in the approach passages to the inner circle of orifices. In burner NA7 these orifices were drilled into an annular channel normally; in burner NA12 they were fed through individual drilled passages with elbow approach to the orifice.

In order to ascertain the precise reason for the difference in spray performance, a single orifice flow test piece, Fig.2, was made up, reproducing the elbow approach condition as to the inner circle of orifices of burner NA12 and also allowing straight approach to the orifice. The observations on water flow through this test piece proved rather interesting and certain points that should be considered in the design of impinging jet type burners were underlined. An explanation of the difference in spray performance between the burners was found. Although perhaps, in general, nothing previously unknown was discovered, it was considered worthwhile to record the findings of this investigation for the benefit, specifically, of rocket motor designers.

2 Experimental procedure

For straight approach the water inlet to the test piece was at A, Fig.2, and the pressure gauge was screwed in at B. For elbow approach the positions of the water inlet and the pressure gauge were reversed. In all cases the jet was directed vertically downwards.

Flow rates were measured over a wide range of injection pressures and the jet was photographed at pressures of 10, 50, 100 and 400 lb/sq in (gauge). Note that the injection pressures used on rocket burners of this type are usually of the order 100 to 140 lb/sq in (gauge). The exit temperatures of the water were recorded.

The diameter of the orifice was 0.073 in (Drill No.49). The size and finish were examined by means of a microscope. The tests were repeated for length to diameter ratios of 10, 5 and 2.5, the last being of the same order as the ratios in the burners. In order to reduce the ratio, the surface C of the test piece was machined away.

3 Results and observations

3.1 Flow rates and discharge coefficients

These are related by the expression

$$C_D = \frac{48w}{\pi D^2 \sqrt{2g.\rho.\Delta P}}$$

where C_D = discharge coefficient

w = weight flow rate in lb/sec

D = diameter of orifice in inches

g = acceleration due to gravity in ft/sec^2

ρ = density of liquid in lb/cu ft

ΔP = injection pressure in lb/sq in (gauge)

The results are recorded in Appendix I. The curves of flow rates and, therefore, of discharge coefficients against injection pressures were similar for all the tests, Figs.3a and 3b. They shewed an initial sharp rise, followed by a drop of some 15 to 18% to constant values of discharge coefficient between 0.63 and 0.68. The discharge coefficients increased slightly with decrease of the L/D ratio, owing to the reduction in frictional loss in the shorter orifices. The lower discharge coefficients for elbow approach were ascribed to the elbow loss.

3.2 Jet deflection

In all the tests, the jet made an angle with the axis of the orifice in the plane of the orifice and approach passage, but was in line with the axis in the plane normal to the former plane. The angles for L/D ratios of 10, 5 and 2.5 were respectively about 1°, 2°, and between 5° and 6°. As can be seen from Fig.4 and 5, these angles were not affected by the method of approach and very little by the injection pressure, the angle increasing slightly in each case with increasing injection pressure from a minimum at the transition point, Fig.6.

3.3 Jet dispersion

On gradually increasing the injection pressure from zero, it was observed that the jet became more dispersed, until at a certain pressure it suddenly contracted into a smooth rod of liquid. Further increase of pressure caused the jet again to become more ragged, until finally disintegration was occurring at or very close to the exit from the orifice. The spray was not, however, a cone of circular section but was elliptical in section, the major axis being in the plane of the orifice and approach passage, see Fig. 4 and 5. The transition to a rod-like jet was associated with the abrupt drop in the discharge coefficient mentioned in para.3.1. When reducing the pressure in the region of the transition pressure, the reverse change in the jet was not seen to occur and there was no discontinuity in the discharge coefficient curve, see Fig.6. Thus, at pressures below the transition pressure, the discharge coefficient curves for increasing and decreasing injection pressures did not coincide, see Fig.3b.

4 Discussion

4.1 Jet deflection

As there was no difference in deflection for the two different methods of approach, straight or elbow, it was deduced that the deflection of the jet was due to the entry face not being normal to the axis of the orifice. The probable pattern of flow in the orifice is shewn in Fig.7a. Corroborative examples from Hauschildt[1] are reproduced in Fig.7b. With the larger L/D ratios, the deflection might be expected to be reduced because of the increased directive effect of the orifice walls.

In check tests with the entry face cut normal to the orifice axis, the jet was not deflected from the line of the orifice axis; this verified the deduction above, see para.5.

4.2 Jet dispersion

Since the entry face was not normal to the orifice axis, the sharp edge where the orifice was drilled through that face was elliptical, not circular. The centre line of the jet stream through the entry section would not be either along the line of the orifice axis or normal to the entry section, but at some intermediate angle, as in Fig.7a. The jet stream, in addition to making an angle with the orifice axis, would also be to some extent elliptical in section. The edges of the jet across the major axis would, therefore, first contact the walls of the orifice. It was considered that this was the reason for the uneven dispersion of the emergent jet.

4.3 Discharge coefficients

Although the injection passage has been referred to as an "orifice", in actual fact it should more correctly be termed a "short tube". At low injection pressures, the short tube runs full with discharge coefficients of the order of 0.80 or more, i.e. discharge coefficient is the product of velocity and contraction coefficients, the latter having its maximum value of unity in the case of a short tube running full[2]. Above a certain pressure, the jet springs away from the walls of the tube and when there is a sharp edged entry the tube then discharges as a sharp edged orifice, with a contraction coefficient less than unity. It is generally stated that the maximum pressure at which a short tube runs full is equal to the atmospheric pressure divided by the velocity coefficient. The transition pressures in the present tests were higher than this value, as also were the values reported by Ward[3], Bird[4], and Kuettner[5]. The values of Reynolds number at which transition occurred in the present work and as given by Ward and Bird are shewn respectively in Figs.8a, 8b and 8c. Adopting Ohnesorge's[6] method of plotting Reynolds number against another dimensionless parameter Z, see Appendix II and Fig.9, it was found that the transition points recorded by the above workers and the authors of this paper lay on a straight line, which in fact almost coincided with Ohnesorge's line marking the initiation of the final stage of jet disintegration. It should be noted that the dimensionless parameters Reynolds number and Z characterise the flow and the physical properties of the liquid respectively. The transition point appears to be that at which the inertia forces in the stream overcome the restraining forces of viscosity and surface tension.

From the straight line plot of Fig.9, it should be allowable to predict the transition pressure for any given combination of liquid and orifice diameter. This has been done, see Appendix II, for water and some liquid rocket propellants with the results plotted in Fig.10. Z was calculated for different values of orifice diameter and liquid properties, and the corresponding values of Reynolds number taken from Fig.9; injection pressures were then calculated assuming a discharge coefficient of 0.65. From the available references, it would appear that the validity of the plot in Fig.9 may be limited to orifices with L/D ratios of less than 1 and between about 2.5 and 6.5.

5 Further tests and discussion

The orifice in the test piece was drilled out to about $\frac{1}{4}$ in. diameter, in order that plugs with drilled orifices could be inserted for test. Flow tests were carried out with the orifices shewn in Fig.11. These orifices

had a common diameter of 0.073 in. and L/D ratio of 2.5. In every case, the entry face was normal to the orifice axis and differed only in the treatment of the entry edge.

In all cases, the issuing jet was clean for straight approach and dispersed but not deflected for elbow approach. Plotting discharge coefficients against injection pressures, as in Fig.11, the discharge coefficients for elbow approach were slightly higher than for straight approach, the curves converging at increased pressures and actually crossing in the case of the orifice with rounded entry. The latter orifice gave the highest values of discharge coefficients and the graph of discharge coefficient against pressure showed no discontinuity. The other entry forms in order of descending discharge coefficients were:- countersunk by centre drill (angle 60°), countersunk by twist drill (angle 110°) and sharp-edged. The discontinuity became more marked in the same order. It should be noted that no accurate measurements were made of the contouring of the entry edges; the operations were carried out as they might be in the manufacture of a rocket burner, the contouring being judged visually.

6 Conclusions

The original purpose of this work was to investigate the reasons for the poor spray characteristics and consequent rough combustion with an impinging jet type rocket burner. The tests described demonstrated that the cause lay in the inclination of the entry face of each individual orifice to the axis of the orifice. This led to dispersion and deflection of the individual jets, resulting in poor impingement, and hence poor atomization and mixing.

Some observations of interest in the design of rocket burners with "short tube" injection orifices were made. The design points underlined are not new, but it was considered useful to restate them for the particular benefit of rocket designers:-

(a) The entry and exit faces of the individual orifices should be normal to the axis of the orifice.

(b) The treatment of the entry edge of the orifice is critical. Preferably this should be carefully radiused. If this is not possible for practical reasons, the treatment of the entry edge, in order of preference, should be, either countersunk by centre drill, or countersunk by twist drill or sharp edged. Clean finish to the bore of the orifice and freedom of the edges from burrs are regarded as absolute essentials.

(c) With any but the rounded entry, there will be a discontinuity in the plot of discharge coefficient against injection pressure. The orifice diameter should be selected so that the required throughput is obtained at an injection pressure remote from the transition pressure, otherwise there is the possibility of pulsating injection. In a rocket motor this would become evident as combustion vibrations.

(d) The method of approach to the orifice proper is also of importance. This should be as direct as possible and of reasonable cross-sectional area compared with the orifice area.

REFERENCES

No	Author	Title, etc
1	Hauschildt	Einfluss der Lage der Ausflussbohrung zur Achse des Zuflusskanals Masch. Lab. der T.H. Dresden, p.22 1942
2	F.C Lea	"Hydraulics", Edward Arnold & Co. p.163
3	F.D. Ward	Fuel injection equipment for gas generators, Part III. The causes of nozzle variations, p.13 C.A.V. Report No. C.29021 1949
4	A.L. Bird	Some characteristics of nozzles and sprays for oil engines. Second World Power Conference, Berlin. Vol.8. Section 29, No.92, p.263 1930
5	Kuettner	Ausflussversuche an Düsen Masch. Lab. der. T.H. Dresden, pp.31-36 1940
6	W.v. Ohnesorge	Die Bildung von Tropfen an Düsen und die Auflösung Flüssiger Strahlen Z.f. angew. Math.u.Mech. Vol.16, pp.355-358 1936
7	V.D.I.	Durchfluss-Messregeln V.D.I. Verlag, G.m.b.H., Berlin 1943

Attached: RP.601 - RP.611

Advanced Distribution

Chief Scientist		Director, RAE	
PDSR (A)		DDRAE (W)	
ADSR (Records)		Guided Weapons	3
DGWRD		Chem. Dept.	
GW.3	6	Armament Dept.	
D Eng RD		Structures Dept.	
Eng RD6		Library	
DGTD (A)			
ERDE Waltham Abbey	6		
ADGW (R & D)			
TPA3/TIB	180		

APPENDIX I

Tabulated Test Results

For the figures tabulated below three measurements were normally made for each set of conditions. With a few explainable exceptions, the consistency in the results was good. The spray times varied from 10 to 60 sec depending on the throughput. The water temperatures as measured were between 14.6 and 15.2°C throughout the tests. A temperature of 15.0°C was assumed when taking values of the physical properties of water for purposes of calculation.

Discharge coefficients were calculated from the following equation:-

$$C_D = \frac{48w}{\pi . D^2 \sqrt{2g . \rho . \Delta P}}$$

where w = weight flow rate, lb/sec

D = diameter of orifice, 0.073 in.

g = acceleration due to gravity, 32.2 ft/sec^2

ρ = density of liquid, 62.4 lb/cu ft

ΔP = injection pressure, lb/sq in (gauge)

$$\therefore C_D = \frac{45.2w}{\sqrt{\Delta P}}$$

TABLE I

Test results for orifice with ratio L/D = 10 (Fig.3a)

Central approach			Elbow approach		
ΔP lb/sq in.	w lb/sec	C_D	ΔP lb/sq in.	w lb/sec	C_D
5	0.036	0.720	7	0.047	0.792
10	0.054	0.772	10	0.056	0.798
20	0.075	0.761	20	0.079	0.797
25	0.083	0.751	30	0.094	0.770
32	0.090	0.735	50	0.101	0.645
45	0.106	0.710	75	0.120	0.640
71	0.126	0.673	125	0.167	0.638
77	0.129	0.662	200	0.199	0.635
118	0.156	0.648	300	0.241	0.628
150	0.175	0.645	400	0.275	0.622
214	0.208	0.645			
300	0.247	0.643			
400	0.283	0.640			

TABLE II

Test results for orifice with ratio L/D = 5 (Fig.3a)

Central approach			Elbow approach		
ΔP lb/sq in.	w lb/sec	C_D	ΔP lb/sq in.	w lb/sec	C_D
5	0.030	0.605	7.5	0.042	0.690
10	0.050	0.715	10	0.049	0.705
20	0.077	0.780	20	0.078	0.785
30	0.097	0.795	35	0.101	0.770
50	0.104	0.665	75	0.124	0.650
100	0.145	0.655	100	0.144	0.650
200	0.207	0.660	200	0.202	0.647
300	0.253	0.660	300	0.248	0.648
400	0.292	0.665	400	0.285	0.645

TABLE III

Test results for orifice with ratio L/D = 5 (Fig.3b)

ΔP lb/sq in.	w lb/sec	C_D	Re
4.8	0.027	0.565	7340
9.0	0.047	0.715	12860
12	0.056	0.730	15320
20	0.077	0.775	21070
30.5	0.094	0.765	25440
40	0.104	0.743	28200
48	0.109	0.712	29600
66	0.117	0.653	31750
80	0.130	0.658	35500
40.5	0.091	0.644	24700
30	0.078	0.644	21330
20	0.064	0.642	17520
15	0.055	0.637	15050
9.5	0.043	0.632	11770

The last column (Reynolds number) is required for Fig.8a and is calculated from

$$Re = \frac{v.D}{\nu}$$

where ν = kinematic viscosity, 1.225×10^{-5} ft^2/sec for water at 15°C

v = jet velocity

Now as

$$v = \frac{w.4}{\rho\ D^2.\pi}$$

then

$$Re = \frac{4}{\rho.D.\pi.\nu}\ w$$

$$= 2.745 \times 10^5\ w$$

TABLE IV

Test results for orifice with ratio L/D = 2.5 (Fig.3a)

Central approach			Elbow approach		
ΔP lb/sq in.	w lb/sec	C_D	ΔP lb/sq in.	w lb/sec	C_D
5	0.029	0.585	5	0.038	0.765
10	0.049	0.705	12	0.054	0.705
15	0.065	0.757	15	0.056	0.652
30	0.083	0.685	30	0.079	0.653
50	0.108	0.690	47	0.098	0.648
70	0.129	0.695	100	0.142	0.643
100	0.154	0.694	200	0.199	0.638
150	0.183	0.678	300	0.244	0.637
200	0.213	0.680	400	0.281	0.635
300	0.261	0.681			
400	0.300	0.677			

APPENDIX II

Calculations for Fig.8, 9 and 10

TABLE V

Calculations of Reynolds number and number Z (Fig.8, 9 and 10)

Worker	Ward (Ref.3)	Bird (Ref.4)	Kuettner (Ref.5)	V.D.I. (Ref.7)	Authors
Liquid	Heavy Kerosene	Light Diesel Oil	Water	Water	Water
D mm in	2.5 0.099	0.33 0.013	1.5 0.059	50 1.97	1.854 0.073
t, °C	15	15	14.5	15	15
$10^4\eta$, $\frac{kg.sec}{m^2}$	2.605	4.90	1.17	1.17	1.17
$10^6\nu$, $\frac{m^2}{sec}$	3.10		1.15	1.15	1.15
$10^4\sigma$, $\frac{kg}{m}$	27.0	32.1	74.5	74.5	74.5
ρ, $\frac{kg}{m^3}$	825	860	1000	1000	1000
10^{-4}.Re	1.0	0.3	2.3	10.0	2.96
10^3.Z	1.10	50.8	3.07	0.50	6.67

D = diameter of orifice

t = temperature of liquid

η = dynamic viscosity of liquid

ν = kinematic viscosity of liquid

σ = surface tension of liquid

ρ = density of liquid

$Re = \frac{v.D}{\nu}$ = Reynolds number

where v = mean jet velocity,

and $Z = \frac{\eta}{\sqrt{\sigma . \frac{\rho}{g} . D}}$

where g = acceleration due to gravity.

TABLE VI

Calculations for Fig.10

Liquid	t	D		$10^4\eta$	$10^6\nu$	$10^4\sigma$	ρ	$10^3 Z$	10^{-4} Re	ΔP (gauge)	
	°C	mm	in	$\frac{kg\ sec}{m^2}$	$\frac{m^2}{sec}$	$\frac{kg}{m}$	$\frac{kg}{m^3}$	-	-	$\frac{kg}{cm^2}$	$\frac{lb}{in^2}$
Water	0	1	0.039	1.824	1.789	77.0	1000	6.52	1.45	8.08	115
		2	0.079	"	"	"	"	4.61	1.90	3.48	49.5
		4	0.157	"	"	"	"	3.21	2.50	1.51	21.5
	20	1	0.039	1.025	1.006	73.5	"	3.74	2.25	6.16	88
		2	0.079	"	"	"	"	2.65	2.95	2.67	38
		4	0.157	"	"	"	"	1.87	3.87	1.13	16.1
W.F. Nitric Acid (98%)	0	1	0.039	1.23	0.789	44.9	1530	4.65	1.90	4.25	60.5
		2	0.079	"	"	"	"	3.29	2.50	1.90	27
		4	0.157	"	"	"	"	2.33	3.30	0.84	12
	20	1	0.039	0.91	0.595	41.7	1505	3.61	2.30	3.50	49.8
		2	0.079	"	"	"	"	2.55	3.10	1.48	21
		4	0.157	"	"	"	"	1.81	4.00	0.64	9.1
Hydrogen Peroxide (80%)	20	1	0.039	1.31	0.96	76.5	1345	4.04	2.15	6.91	98.5
		2	0.079	"	"	"	"	2.84	2.80	2.93	41.7
C-Fuel	20	1	0.039	~1.4	~1.59	28.6	921	8.54	1.22	3.66	52.1
		2	0.079	"	"	"	"	6.04	1.58	1.54	21.9
Kerosene	0	1	0.039	2.70	3.25	25.5	814	18.56	0.68	4.79	60.4
		2	0.079	"	"	"	"	13.14	0.88	1.99	28.3
	20	1	0.039	1.81	2.18	24.5	802	12.80	0.90	3.30	52.6
		2	0.079	"	"	"	"	9.05	1.18	1.41	22.7

SECRET

SECRET

Example: Liquid: Water
Orifice Dia.: 1 m.m.
Liquid Temp.: 20°C

(1) Calculate Z from values of physical properties of liquid

$$Z = \frac{\eta}{\sqrt{\sigma \cdot \frac{\rho}{g} \cdot D}} = \frac{1.025 \times 10^{-4}}{\sqrt{73.5 \times 10^{-4} \times \frac{1000}{9.81} \times 10^{-3}}} = 3.74 \times 10^{-3}$$

(2) Take R_e for transition point for number Z from Fig.9

$$R_e = 2.25 \times 10^4 = \frac{v.D}{\nu} = \frac{C_D \sqrt{2g \frac{\Delta P}{\rho}} \times D}{\nu}$$

(3) Calculate ΔP from R_e, assuming $C_D = 0.65$

$$\Delta P = \left(\frac{R_e \cdot \nu}{C_D \cdot D}\right)^2 \frac{\rho}{2g} = \left(\frac{2.25 \times 10^4 \times 1.006 \times 10^{-6}}{0.65 \times 10^{-3}}\right)^2 \frac{1000}{19.62} = 61{,}600 \ \frac{kg}{m^2}$$

$$= 6.16 \ \frac{kg}{cm^2} = 88 \ lb/in^2$$

FIG.1

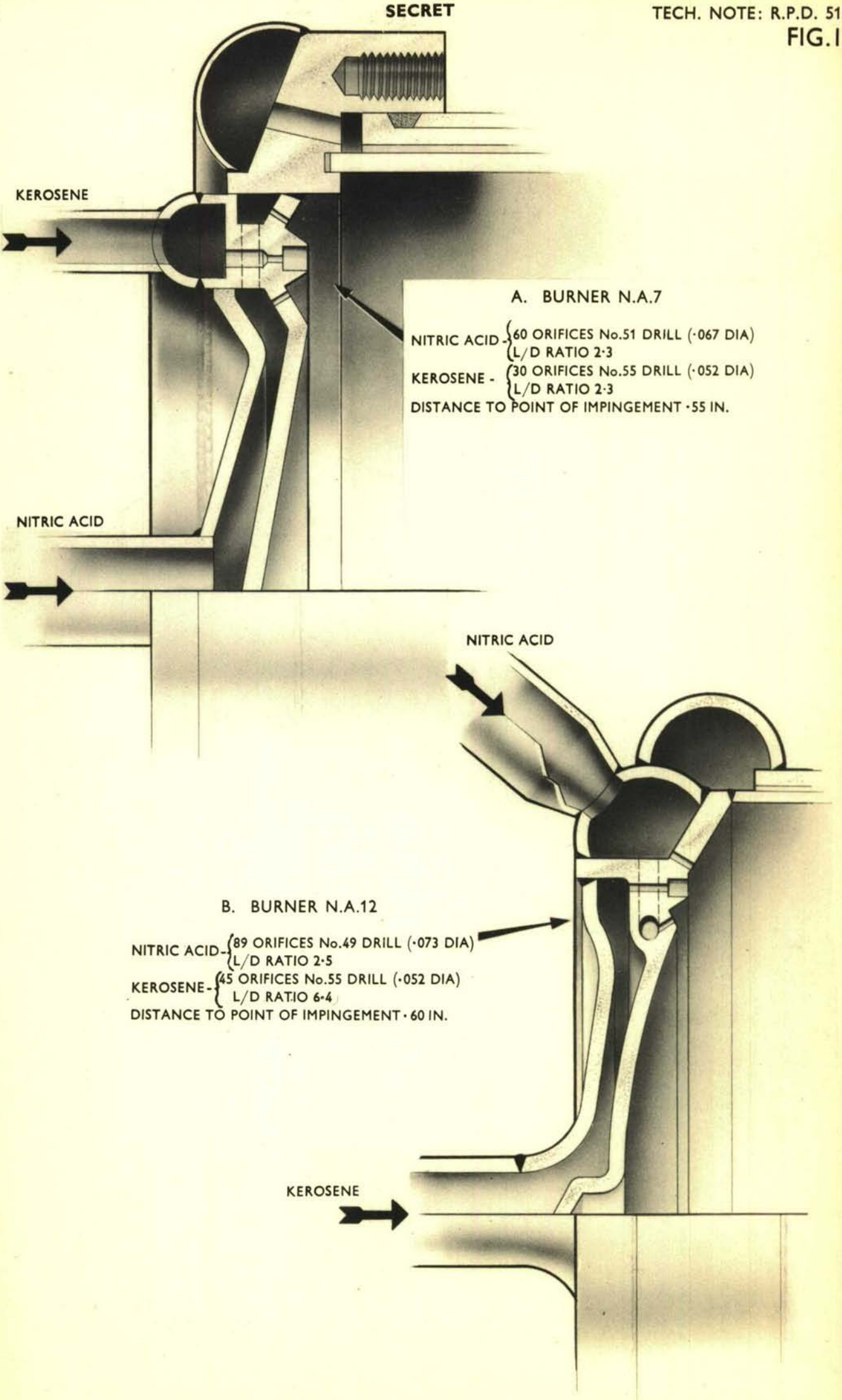

FIG.1. NITRIC ACID - KEROSENE BURNERS

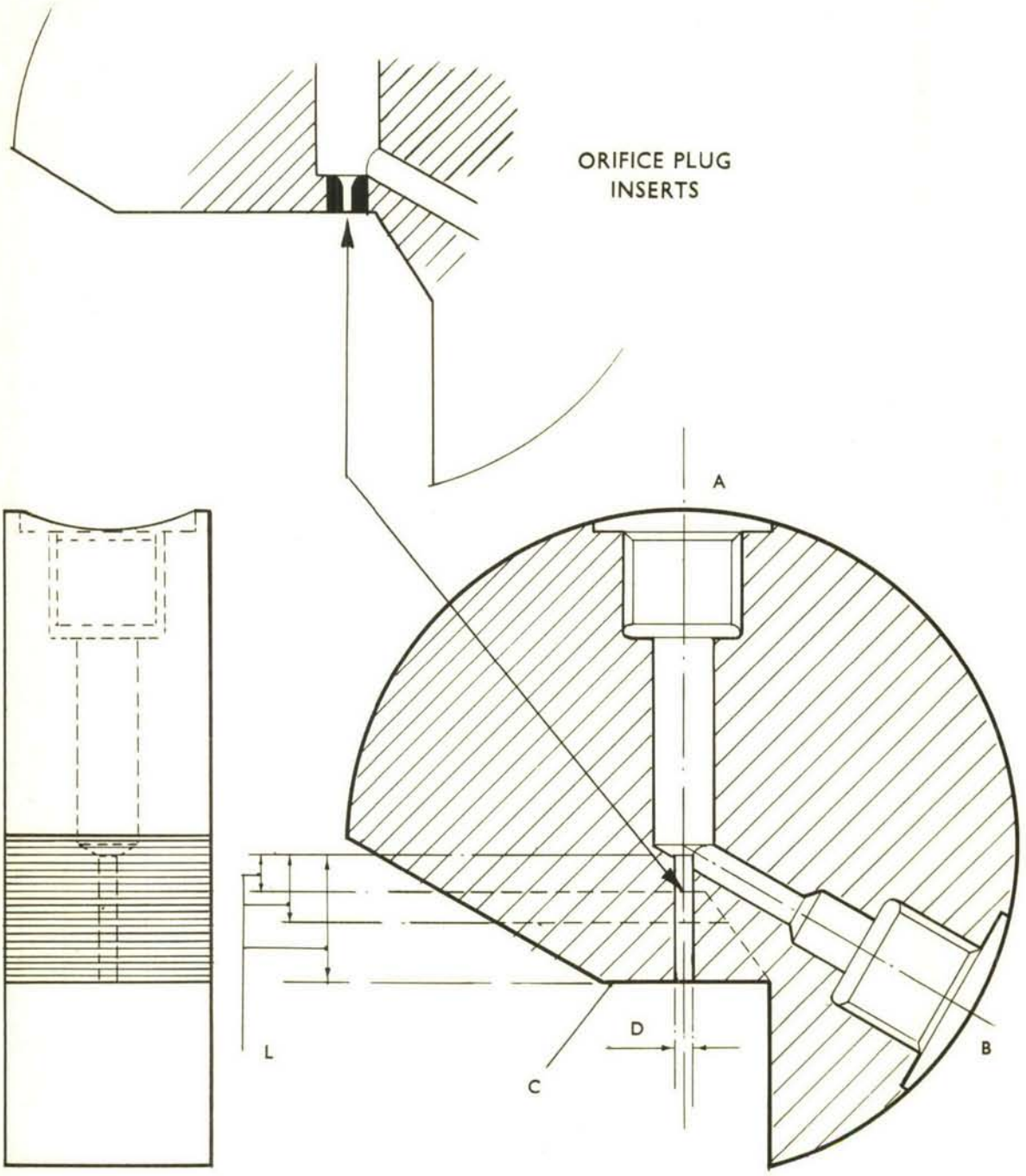

ORIFICE DIAMETER	= 0·073 in.
$\frac{\text{LENGTH}}{\text{DIAMETER}}$ OF ORIFICE	= 10-5-2·5
DIAMETER OF STRAIGHT APPROACH PASSAGE	= 0·375 in.
DIAMETER OF ELBOW APPROACH PASSAGE	= 0·2 in.

FIG.2. TEST PIECE SIMULATING NITRIC ACID ORIFICE AND APPROACH PASSAGES OF BURNER N.A.7 (FIG.1a) OR BURNER N.A.12 (FIG.1b)

FIG.3

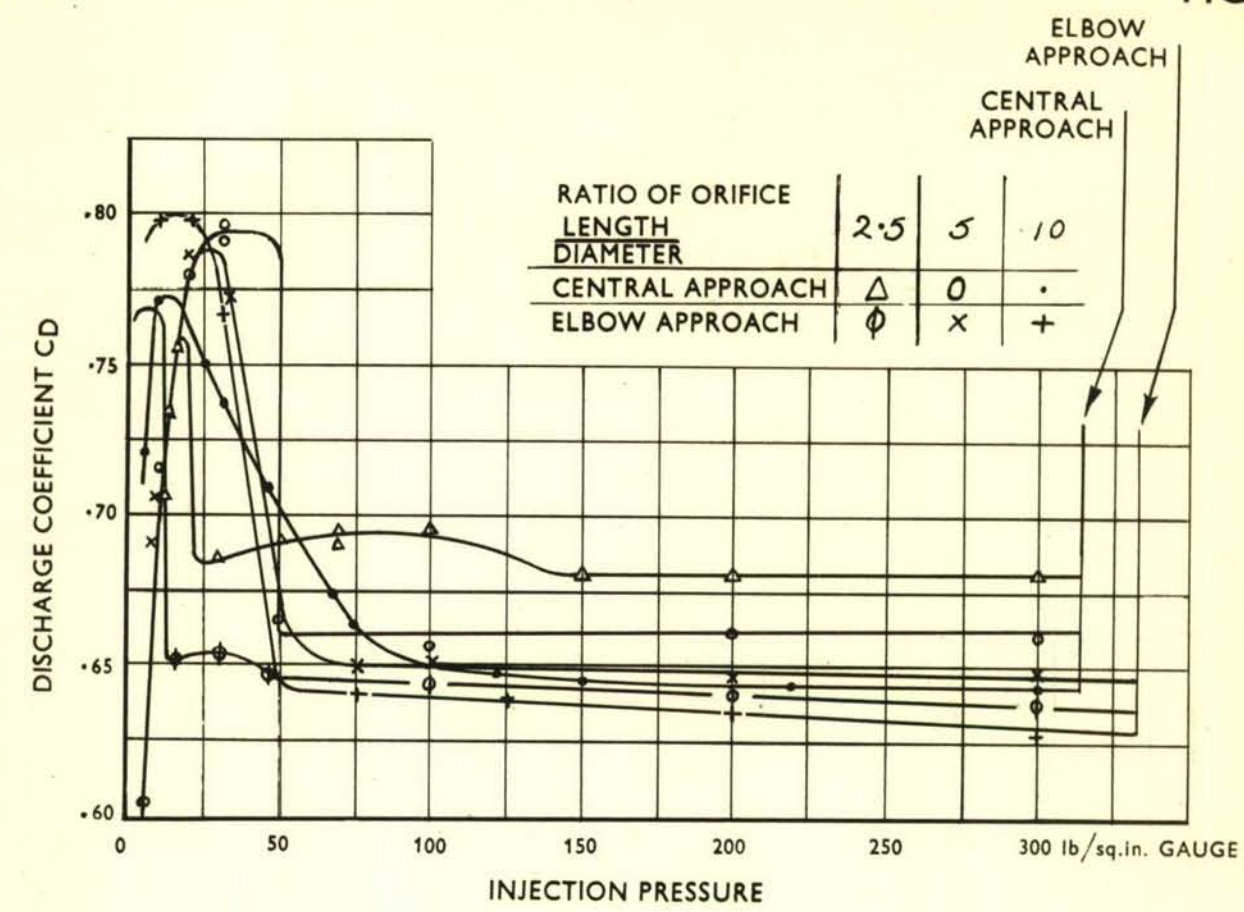

(A) DIFFERENT APPROACHES AND $\frac{\text{LENGTH}}{\text{DIAMETER}}$ RATIOS

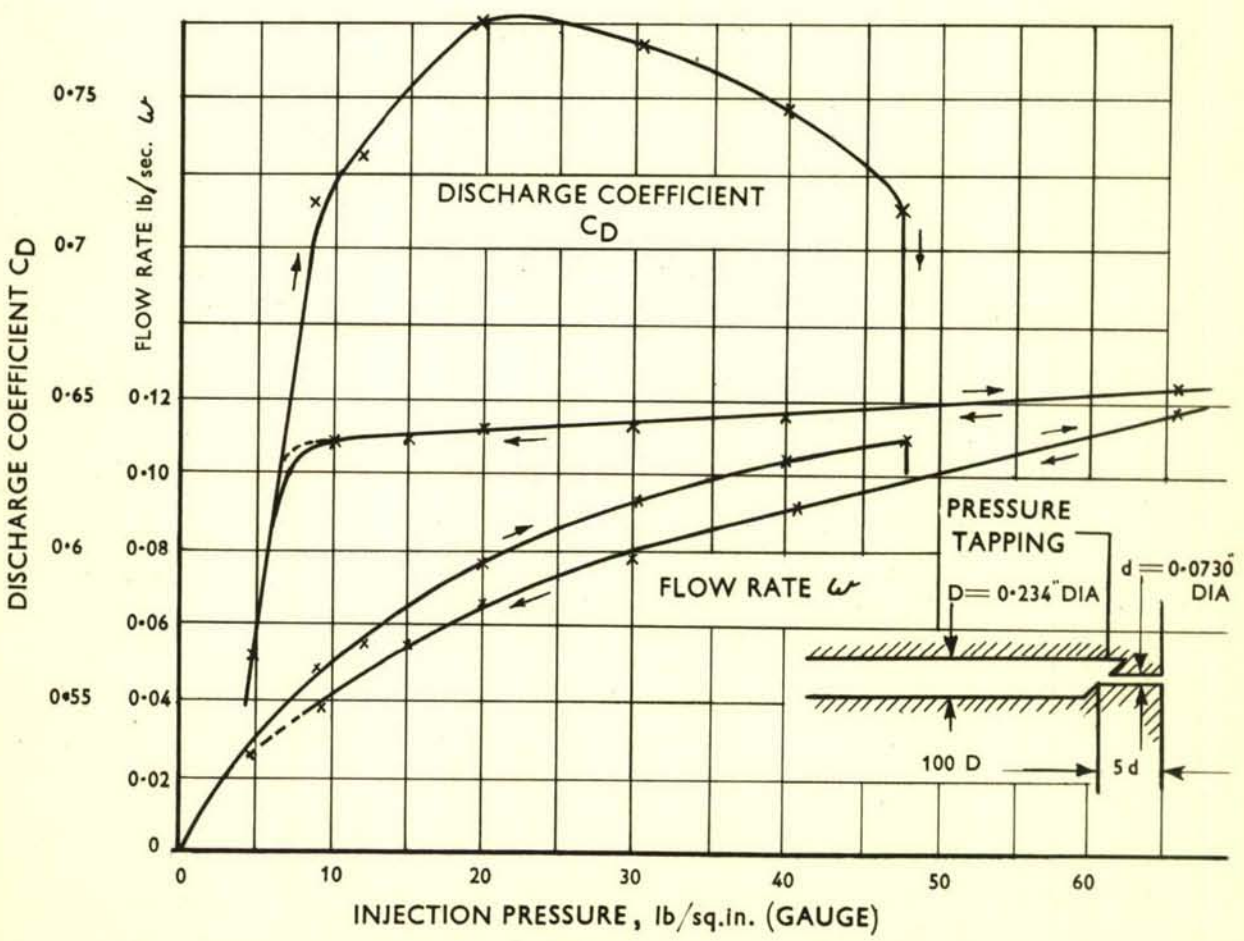

(B) CENTRAL APPROACH $\frac{\text{LENGTH}}{\text{DIAMETER}}$ = 5 NEAR TRANSITION POINT

FIG.3. DISCHARGE COEFFICIENTS AND FLOW RATES AGAINST INJECTION PRESSURES

FIG.4

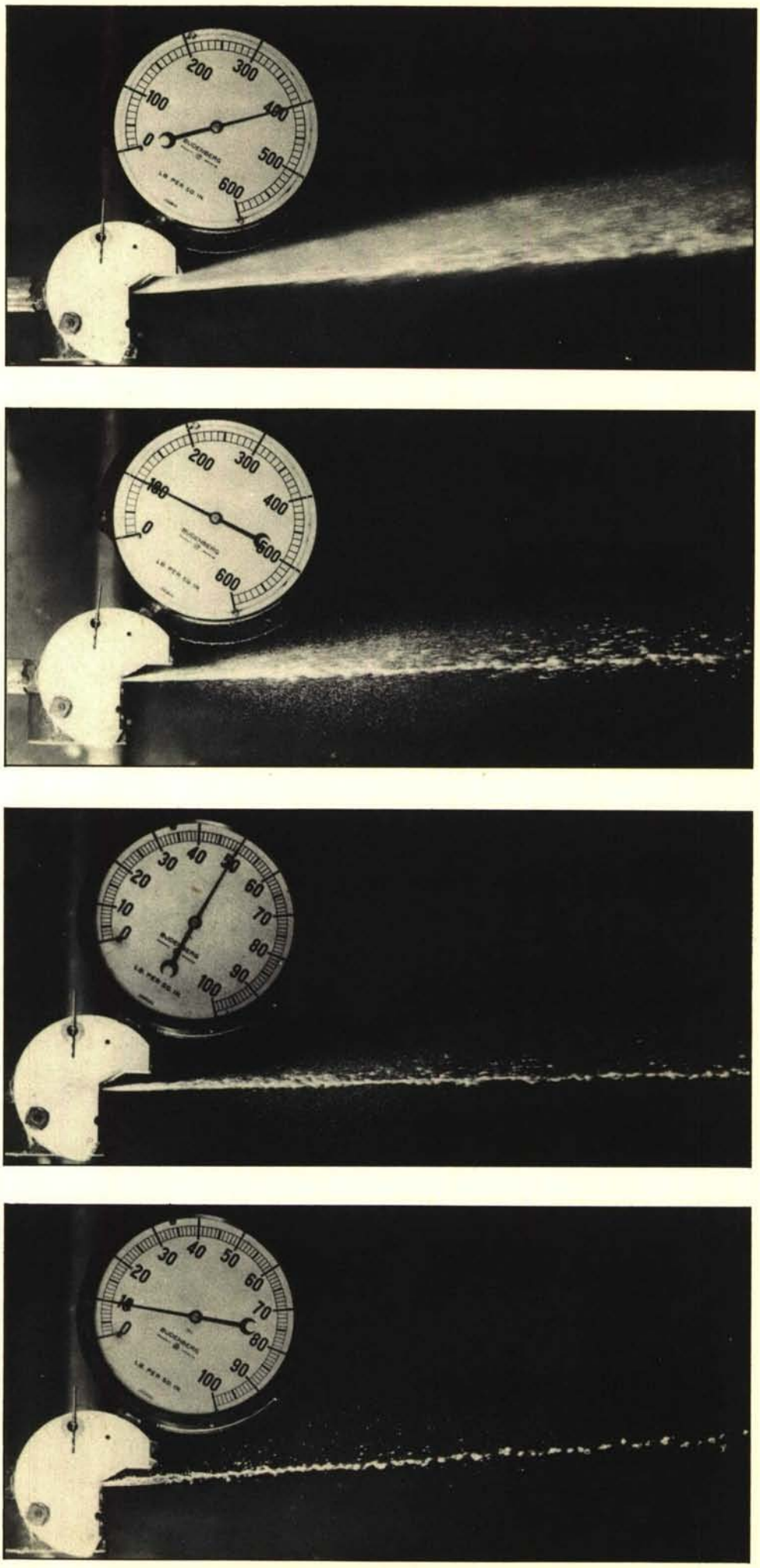

FIG.4. SPRAY PATTERNS AT DIFFERENT INJECTION PRESSURES.
CENTRAL APPROACH ORIFICE $\frac{\text{LENGTH}}{\text{DIAMETER}} = 2{\cdot}5$

FIG.5

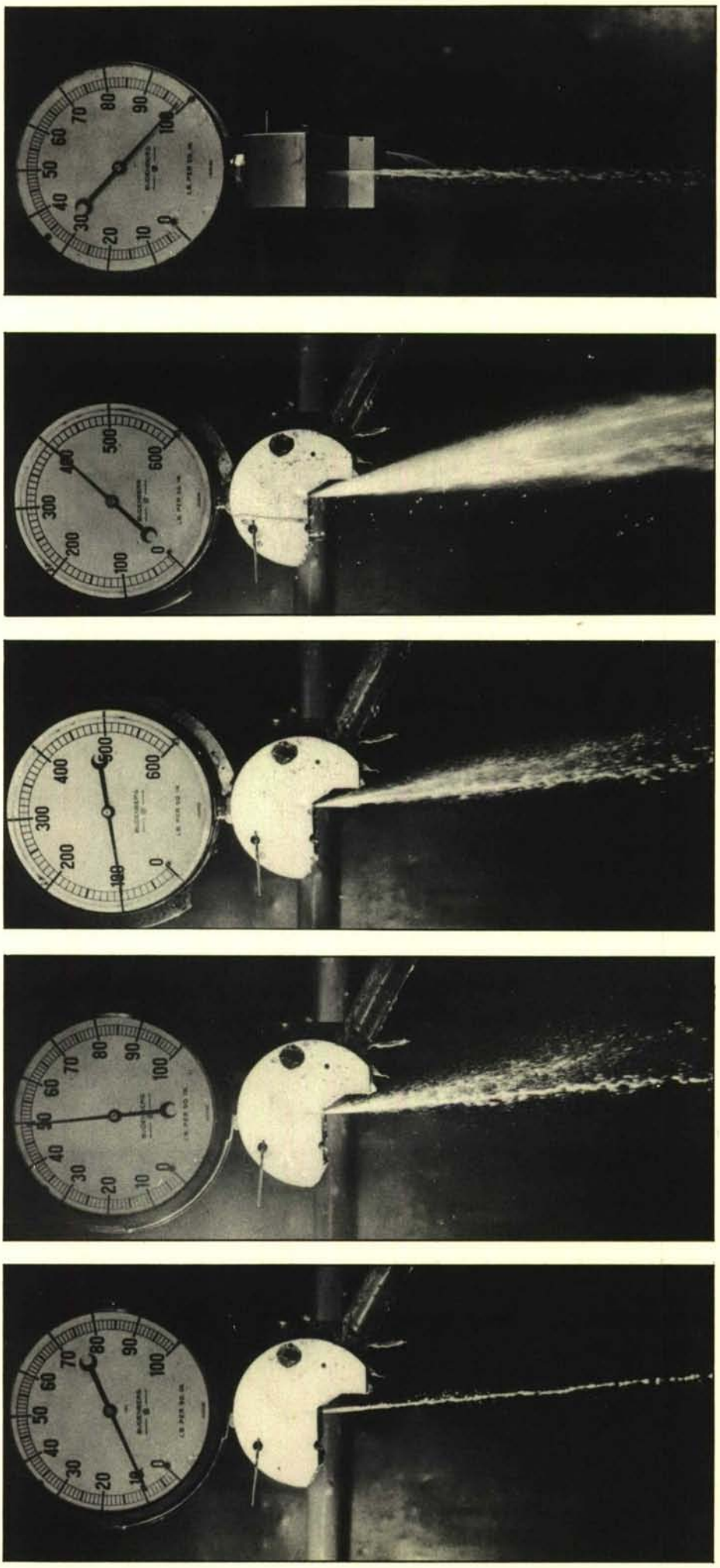

FIG.5. SPRAY PATTERNS AT DIFFERENT INJECTION PRESSURES.
ELBOW APPROACH ORIFICE $\frac{\text{LENGTH}}{\text{DIAMETER}} = 2{\cdot}5$

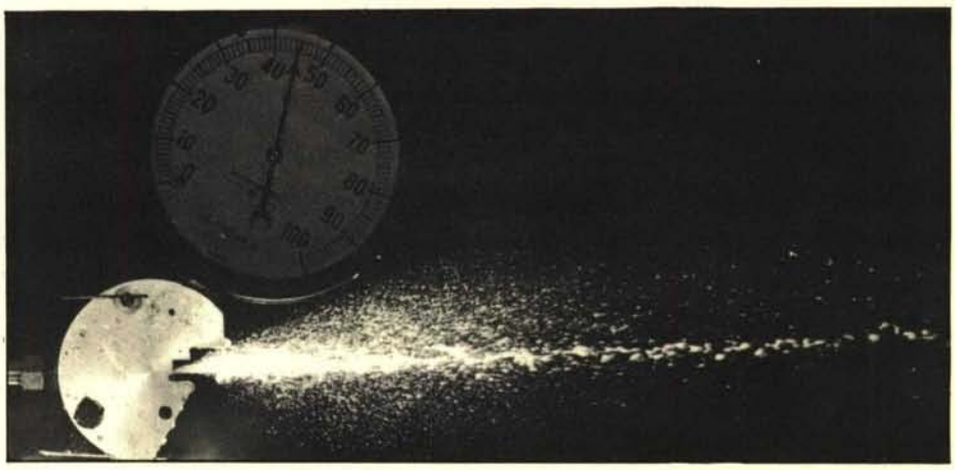

(A) INJECTION PRESSURE RAISED FROM ZERO TO TRANSITION POINT

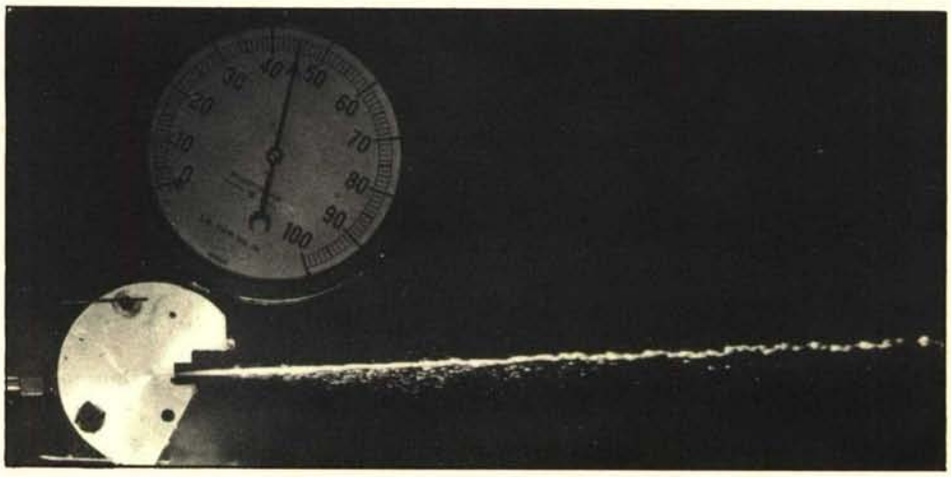

(B) INJECTION PRESSURE DECREASED FROM ABOVE TRANSITION POINT

FIG.6. SPRAY PATTERNS NEAR TRANSITION POINT. CENTRAL APPROACH ORIFICE

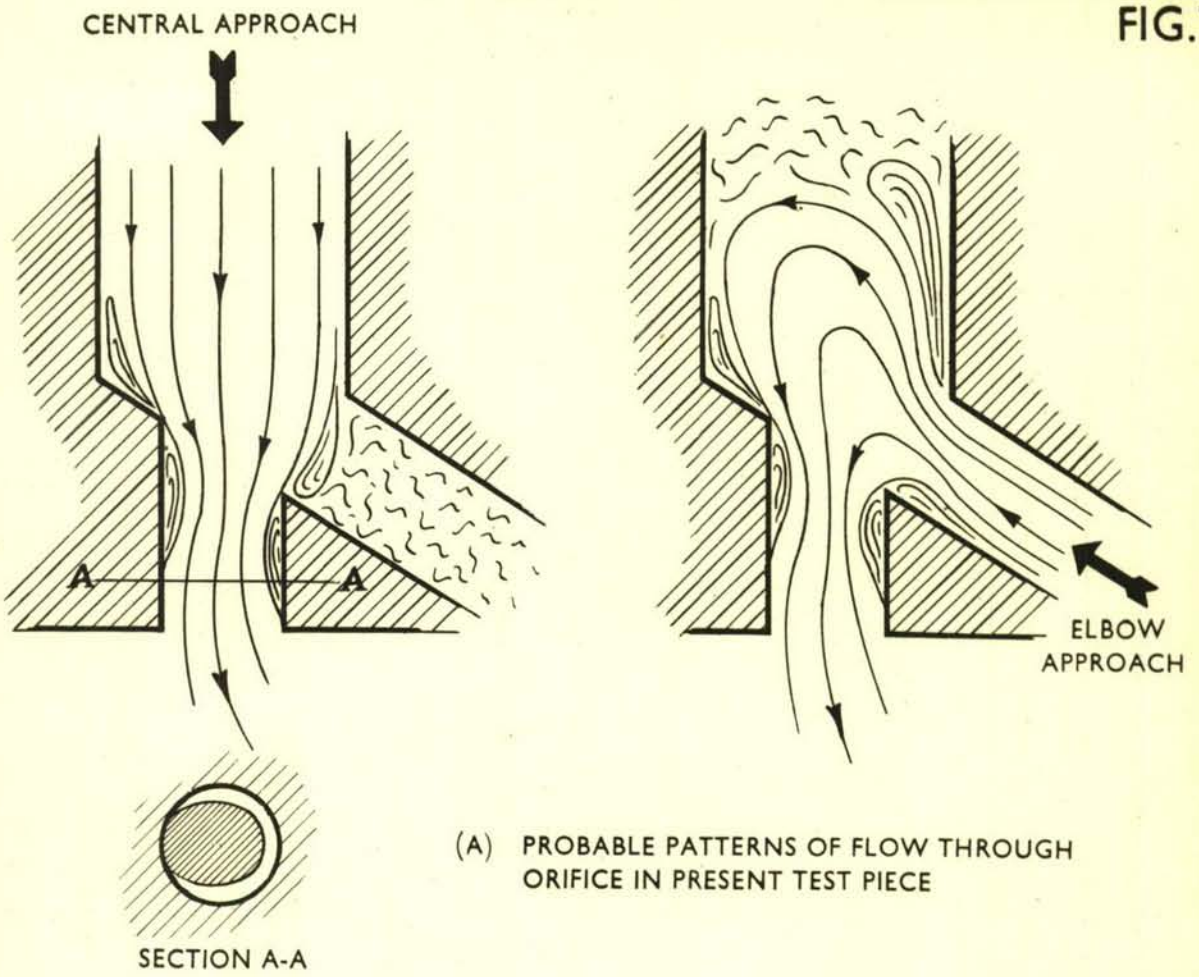

(A) PROBABLE PATTERNS OF FLOW THROUGH ORIFICE IN PRESENT TEST PIECE

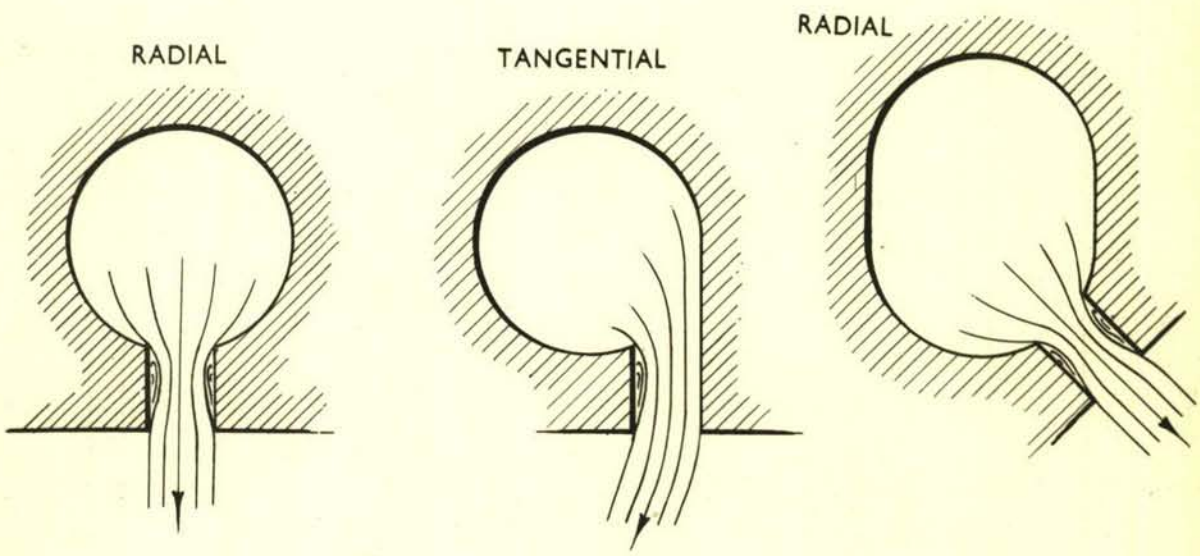

(B) JET STREAMS FROM ORIFICES WITH RADIAL AND TANGENTIAL ENTRY (HAUSCHILDT REF 1)

FIG.7. PATTERNS OF FLOW THROUGH VARIOUS ORIFICES

FIG.8

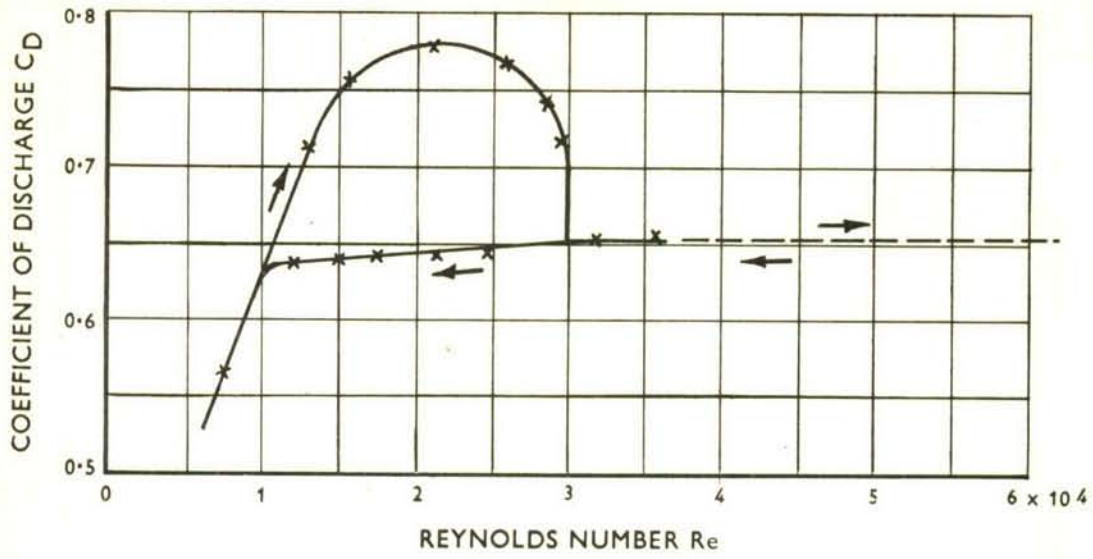

A. COEFFICIENT OF DISCHARGE WITH REYNOLDS NUMBER FOR PRESENT TEST PIECE. CENTRAL APPROACH ORIFICE L/D = 5

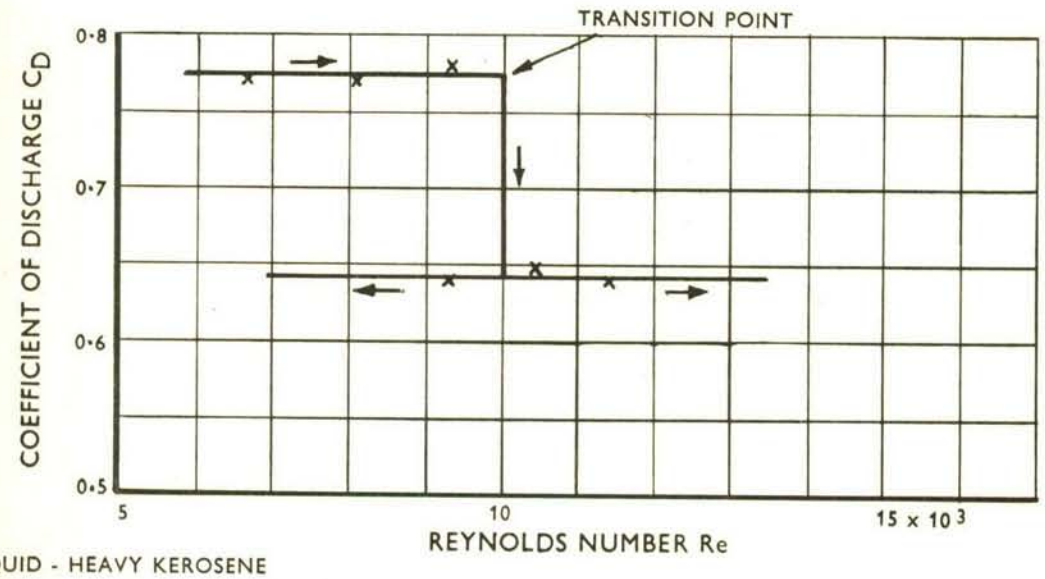

LIQUID - HEAVY KEROSENE
DIA - 2·5 mm.
L/D - 5·0

B. WARDS DATA (REF 3)

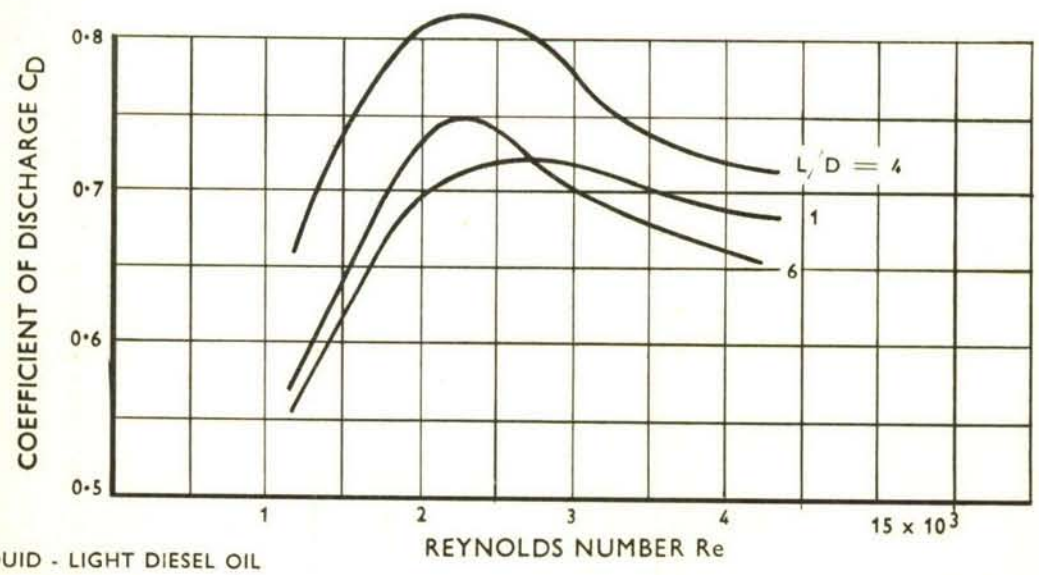

LIQUID - LIGHT DIESEL OIL
DIA - 0·013 in.

C. BIRDS DATA (REF 4)

FIG.8. VARIATION OF COEFFICIENT OF DISCHARGE WITH REYNOLDS NUMBER

FIG.9

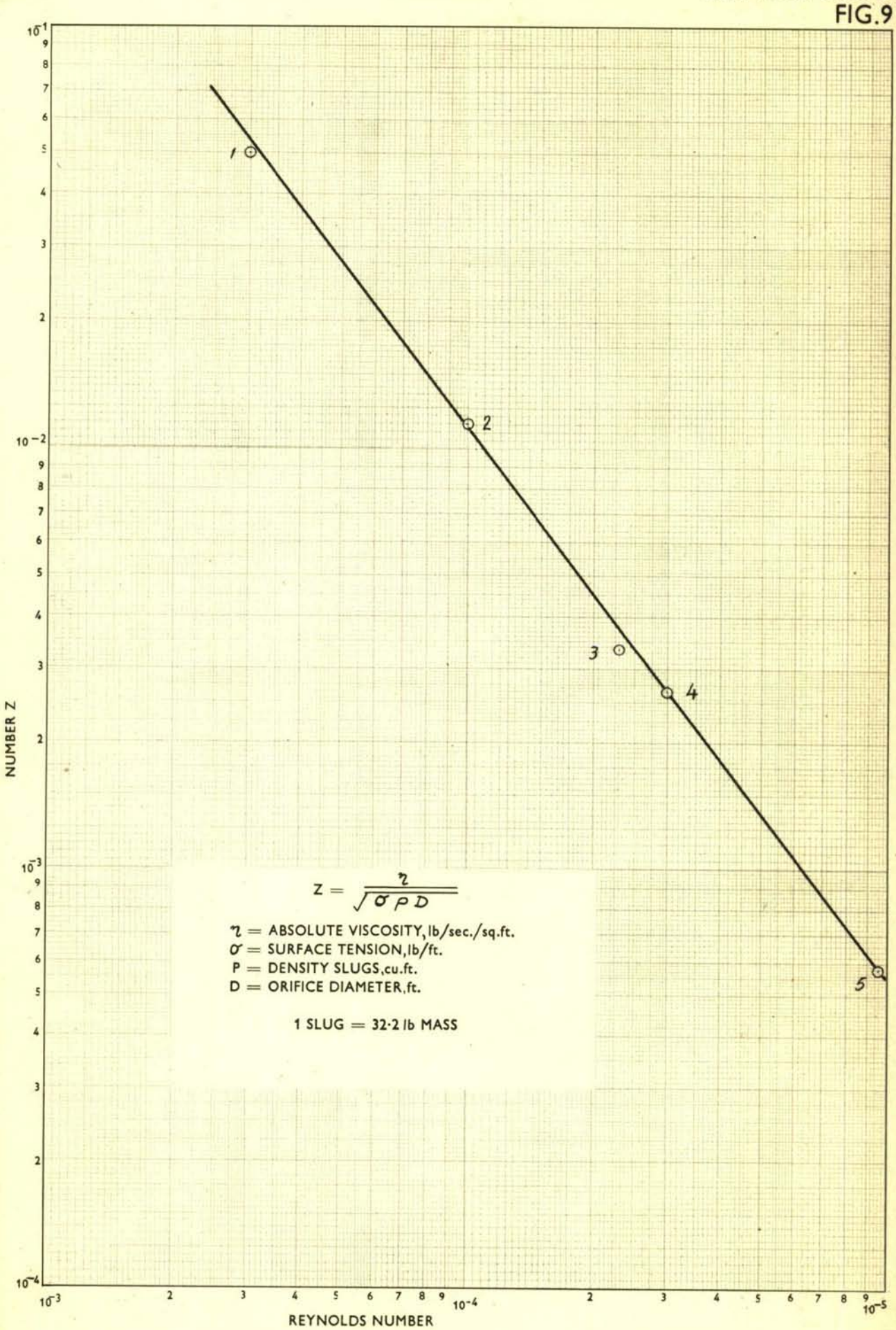

1. BIRD (ref 4)
2. WARD (ref 3)
3. KUETTNER (ref 5)
4. PRESENT WORK
5. GERMAN STANDARD ORIFICE (ref 7)

FIG.9. TRANSITION POINTS PLOTTED WITH CO-ORDINATES Z AND REYNOLDS NUMBER

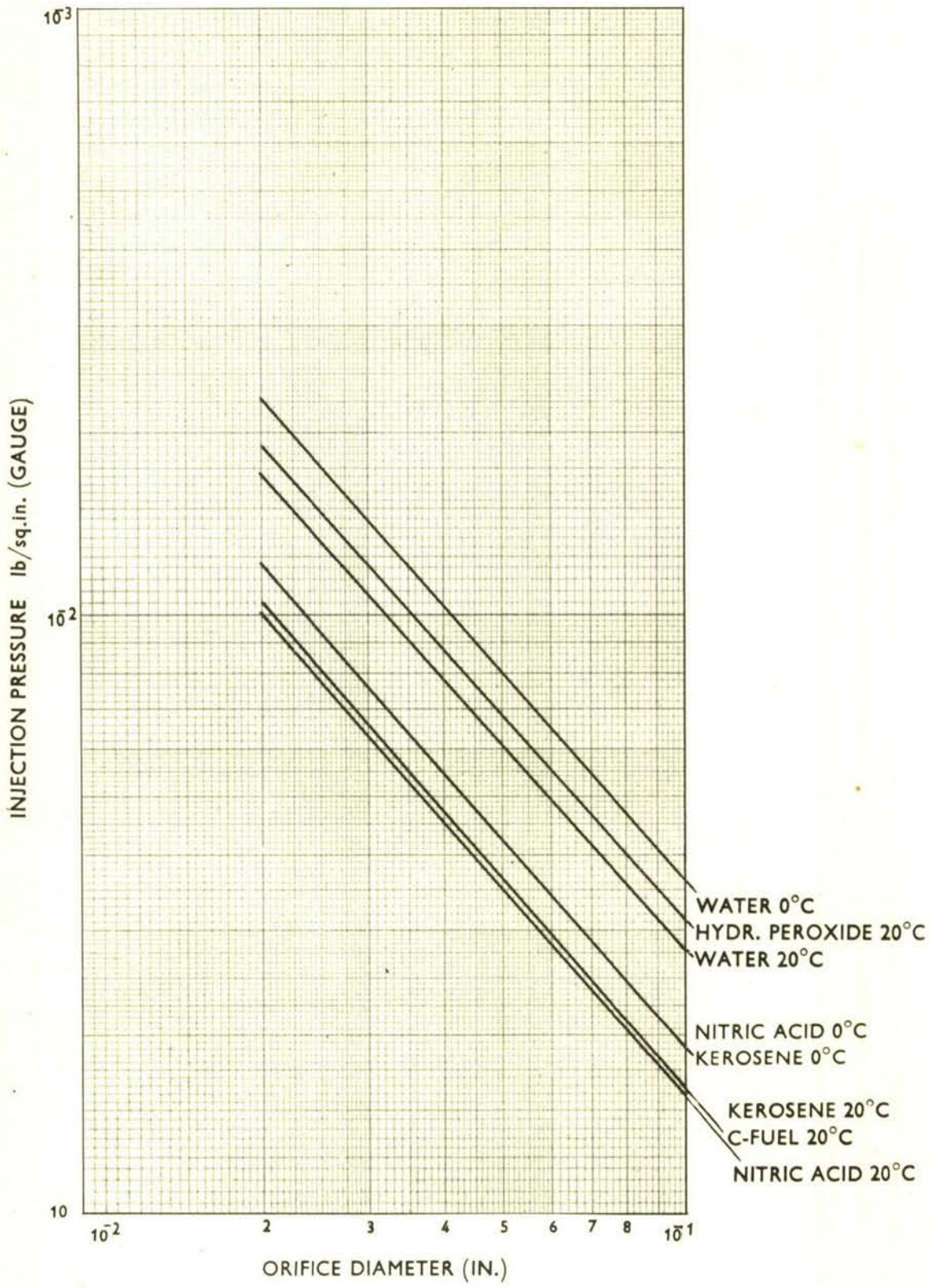

FIG.10. INJECTION PRESSURE AT TRANSITION POINT OF COEFFICIENT OF DISCHARGE FOR DIFFERENT ORIFICE DIAMETERS, LIQUIDS, AND TEMPERATURES

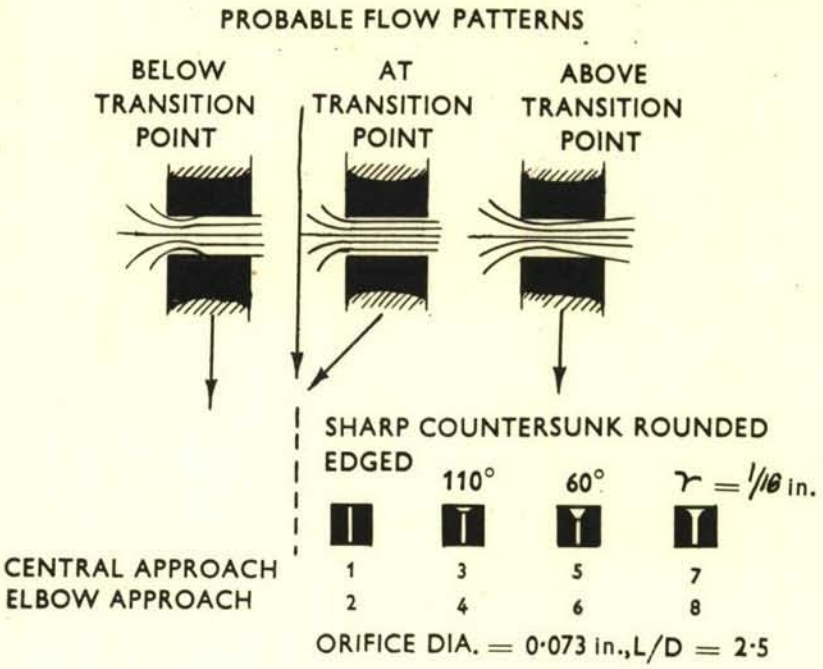

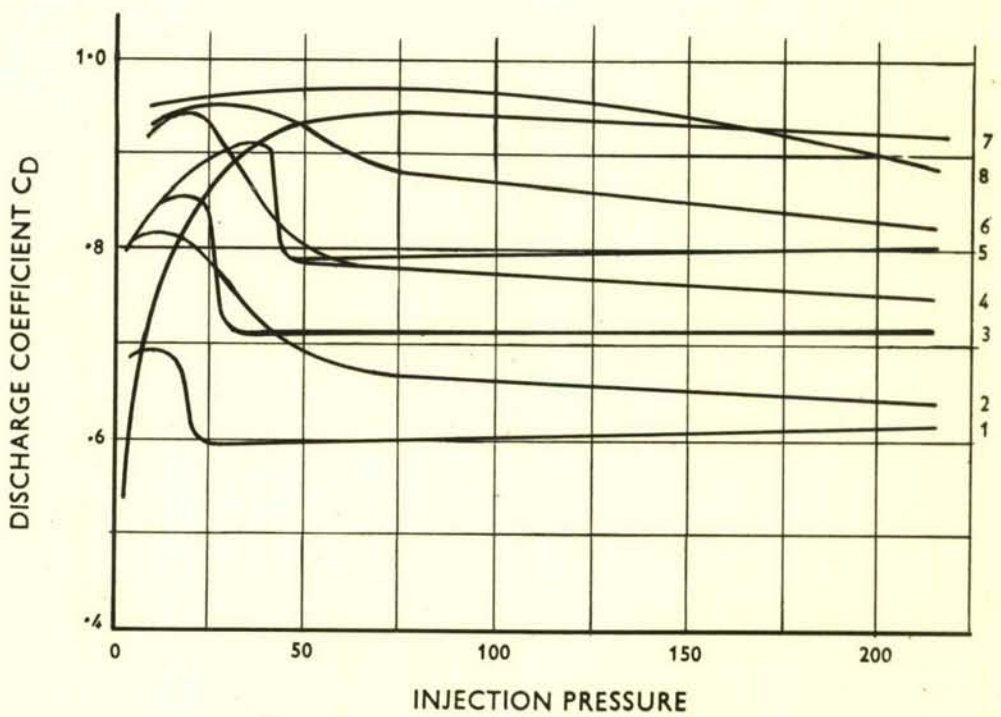

FIG.11. DISCHARGE COEFFICIENTS PLOTTED AGAINST INJECTION PRESSURES FOR DIFFERENT ORIFICE ENTRY SHAPES

~~SECRET~~

~~SECRET~~